Bone Tumors

8

Daniel Vanel, Piero Picci, Catherine Ridereau-Zins, and Marco Gambarotti

Contents

D. Vanel (✉) • P. Picci • M. Gambarotti
Research Department,
The Rizzoli Orthopaedic Institute,
Via del Barbiano 1, 40136 Bologna, Italy
e-mail: daniel.vanel@ior.it

C. Ridereau-Zins
Radiology Department,
CHU Angers, 4 rue Larrey, 49000 Angers, France

Abbreviations

CT   Computed tomography
MRI   Magnetic resonance imaging
PET   Positron emission tomography
STIR   Short tau inversion recovery

8.1 Introduction

In old patients metastases are by far the most frequent lesion. Their detection must be planned carefully and only when the knowledge that is obtained will have therapeutic consequences. Bone scintigraphy, radiographs, computed tomography (CT), magnetic resonance imaging (MRI), and positron emission tomography (PET) all have specific uses and indications. The treatment of some primary bone tumors has been completely transformed by chemotherapy but mainly in young patients. At the same time, surgery has changed and drastic measures, such as amputation, are much rarer. The perfect local staging allows the best choice of indications as well as evaluation of neoadjuvant treatment. Plain film remains the first indispensable diagnostic step, especially for primary tumors. CT improves diagnostic capability, and MRI is the best technique for local staging. PET can evaluate new criteria, but it is still being evaluated.

8.2 Primary Tumors (Figs. 8.1 and 8.2)

8.2.1 Diagnosis

Analysis of bone tumors is statistical, leading to a reasonable probability of a correct diagnosis (Lodwick et al. 1980; Madewell et al. 1981). The radiologist and the pathologist both do the same job but with different tools. The radiologist studies the whole specimen from afar and

the pathologist a small piece from close-up. Combining the two approaches brings the best results, emphasizing the importance of teamwork in providing the best care.

Age is very useful: after 65, the great majority of bone tumors are metastases or myeloma. Diagnosing metastases requires a perfect understanding of how they could change the treatment: in other words if no change in treatment is planned, they should not be looked for, unless they are painful. Among primary tumors, chondrosarcomas are

Fig. 8.1 Bone lesions at the Rizzoli Institute in patients over age 65 (Istituto Ortopedico Rizzoli – Laboratory of Experimental Oncology – Section of Epidemiology – Bologna, Italy)
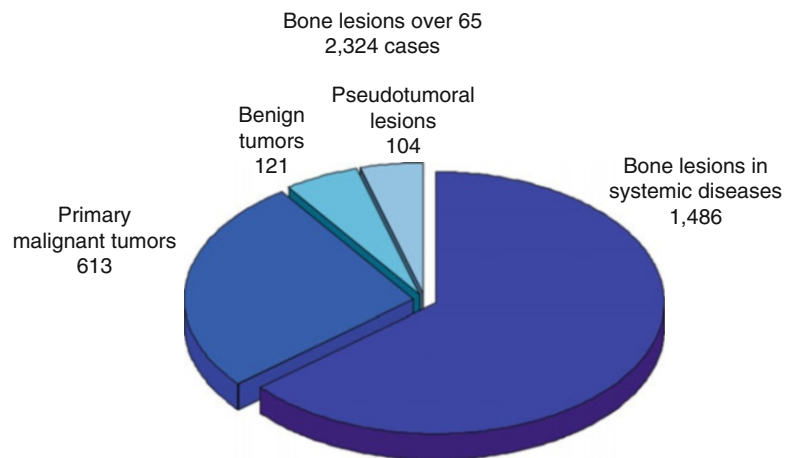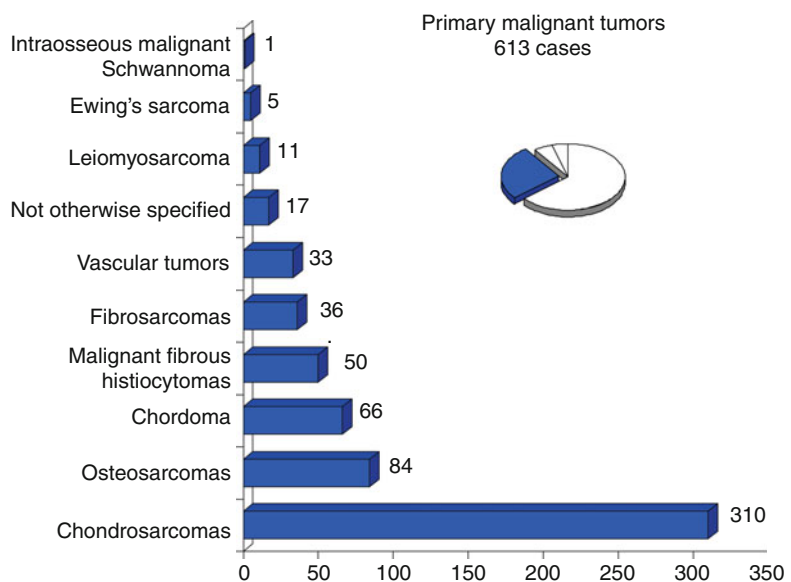

Fig. 8.2 Primary malignant bone tumors in patients over age 65 (Istituto Ortopedico Rizzoli – Laboratory of Experimental Oncology – Section of Epidemiology – Bologna, Italy)

the most frequent. Location helps: adamantinoma involves the anterior cortex of the shaft of the tibia, and in the epiphysis, giant cell tumor is a logical guess. Size is also helpful as small lesions are often benign. The lesion can be centered on the middle of the medullary cavity, often eccentric, rarely on the cortex or periosteum.

The matrix can be lytic, calcified, or ossified. Popcorn calcifications indicate cartilage (with nodules calcified at the periphery or in between them). The shape of periosteal bone formations indicates the mode of growth of the tumor. When thick, they indicate slow growth, perpendicular to the main axis of the bone, almost always malignant. A Codman triangle indicates a longitudinal periosteal reaction broken by tumor progression in its center. Cortical destruction and soft tissue involvement indicate aggressiveness. A thin calcified periosteal formation limiting the lesion indicates slow growth, even if the cortex has disappeared, and is probably a benign lesion. Conversely, tumor on both sides of a not yet destroyed cortex is a good sign of aggressiveness (Glass et al. 1986).

The radiologist must then, usually on radiographs first, diagnose the "leave me alone lesions," for which nothing more is needed. They are rare in geriatric patients (osteochondromas, hemangiomas, chondromas, fibrous dysplasia) and are discovered incidentally.

If the diagnosis is difficult, because the site is difficult to study, the next step is CT (Regent et al. 1986). It gives better analysis of short and flat bones. Small calcifications, density to characterize water or fat, limited cortical erosions, or soft tissue involvement is better detected. The cartilaginous cuff of an osteochondroma is easily measured (Brown et al. 1986). MR is less useful, visualizing fluid-fluid levels, or the high T2 signal of cartilaginous nodules, or peritumoral edema.

If imaging suggests malignancy, staging should be performed, if possible before biopsy. Biopsy should be performed by a well-trained physician. It is surgical, or radiological, and the tract must be chosen in collaboration with the surgeon. Congelation and tattooing of the tract must be planned when necessary.

8.2.2 Staging

8.2.2.1 Localization
Locating the tumor is done with help of MRI MR (Kenney et al. 1981; Aisen et al. 1986; Bloem et al. 1988; Bohndorf et al. 1986). Medullary extension, and so the level of resection, is analyzed. Skip lesions are detected, as well as the relation to vessels and nerves. The main limitation is the study of the joints: when a tumor abuts on the cartilage, it may be very difficult to detect minimal joint involvement that could change surgery. Radiation therapy fields are best chosen.

8.2.2.2 General Staging
Bone metastases are detected by bone scintigraphy, total-body MRI, or PET, and pulmonary metastases by CT (Schima et al. 1994; Vanel et al. 1984). All nodules are not malignant, and if CT sensitivity is rather good, specificity is quite poor, and treatment is rarely changed by the detection of pulmonary nodules without histological proof. PET is not sensitive to small pulmonary nodules.

8.2.3 Treatment Effectiveness and Follow-Up

Some tumors receive neoadjuvant chemotherapy, but this is rare in geriatric patients. Decrease of peritumoral edema and of early MR uptake after contrast injection is correlated with efficient treatment (Picci et al. 2001; Verstraete et al. 1994; De Baere et al. 1992; van der Woude et al. 1994). After surgery with non-paramagnetic prostheses or fixations (usually titanium), MR can still be performed with few artifacts.

8.2.4 Most Frequent Examples

8.2.4.1 Malignant
- Chondrosarcoma (Fig. 8.3)
- Conventional chondrosarcoma (Murphey et al. 1998; Geirnaerdt et al. 2000; Vanel et al. 2012) is a rather frequent tumor that can only be cured by surgery. Therefore, early diagnosis, clever biopsy tract, and perfect

Fig. 8.3 Different types and frequency of chondrosarcomas in patients over age 65 (Istituto Ortopedico Rizzoli – Laboratory of Experimental Oncology – Section of Epidemiology – Bologna, Italy)
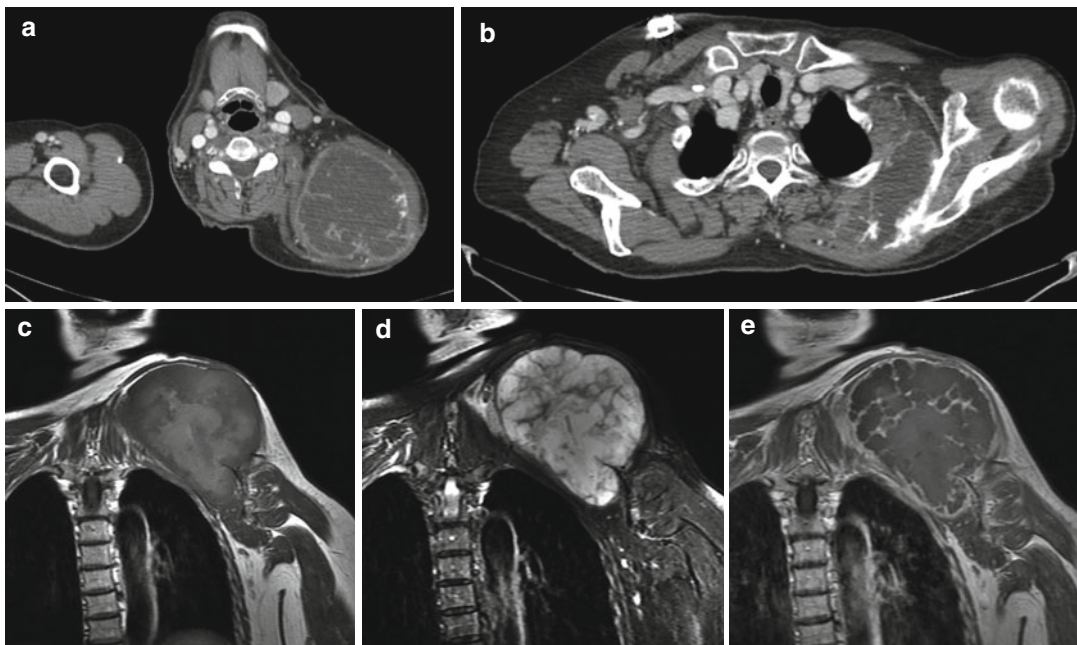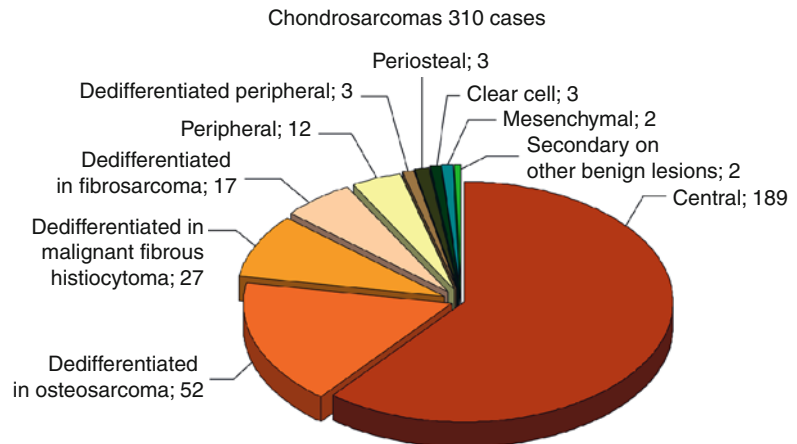
Chondrosarcomas 310 cases

- Periosteal; 3
- Dedifferentiated peripheral; 3
- Clear cell; 3
- Mesenchymal; 2
- Peripheral; 12
- Secondary on other benign lesions; 2
- Dedifferentiated in fibrosarcoma; 17
- Central; 189
- Dedifferentiated in malignant fibrous histiocytoma; 27
- Dedifferentiated in osteosarcoma; 52

Fig. 8.4 Chondrosarcoma of the scapula. Injected CT (**a**, **b**), MRI coronal T1-weighted (**c**), and T2 fat-saturated (**d**) and injected (**e**) images. The tumor has a lobular pattern, hypodense on CT. The lesion starts from the spine of the scapula. It has a high signal and a lobular pattern on T2 images. Only the septae enhance after injection

local staging are mandatory. On radiographs, the lesion is lytic, with typical round calcifications with a clear center, due to calcifications in between the lobules of cartilage or at the periphery of the lobules (Fig. 8.4). Limitation is usually sharp, indicating slow growth. Calcifications are better analyzed on CT, but a precise staging depends on MR. The tumor has a typical high signal on T2-weighted sequences, with no or limited uptake after injection, only around the lobules. Nodules of cartilage separated by fat marrow are often visible at the periphery of the main tumor, confirming the cartilaginous nature of the lesion, and correspond to a benign probably preexisting chondroma.
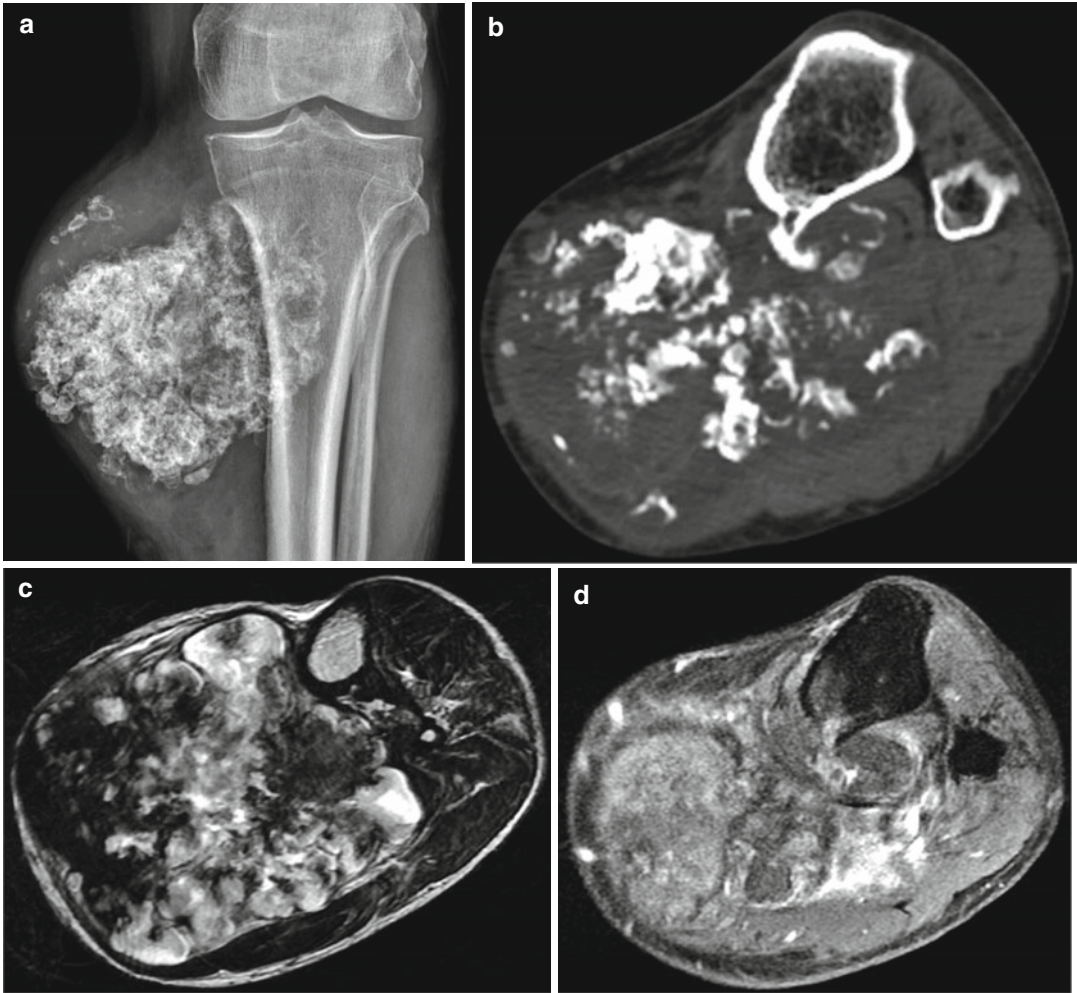
Fig. 8.5 Dedifferentiated peripheral chondrosarcoma of the tibia. On radiograph (**a**) and CT (**b**), typical cartilaginous calcifications, round with a clear center, are well seen. The basis of the osteochondroma is visible on CT. On an axial T2-weighted MRI (**c**), a part of the lesion is made of high-signal lobules, but the lesion is heterogeneous. The dedifferentiated part takes up strongly contrast medium after injection (**d**). The biopsy must be directed at this part

Dedifferentiated chondrosarcoma (Staals et al. 2006, 2007) is revealed radiologically by a completely lucent area, without calcifications. On MR, this aggressive part takes up contrast medium, which helps guide the biopsy. Diagnosing the dedifferentiated part of the tumor is a useful part of the radiological work. Peripheral chondrosarcoma is often diagnosed on new pain or radiological changes of a known osteochondroma. The thick cartilaginous cuff, easily measured on ultrasound, CT, or MR, indicates malignancy. Dedifferentiation is possible but rare (Fig. 8.5).

- Osteosarcoma (Fig. 8.6) can be conventional or often secondary to a preexisting lesion, infarct, Paget disease (Shaylor et al. 1999) (Fig. 8.7), or radiation changes (Fig. 8.8). Soft tissue involvement and cortical lysis indicate fast growth. Fat disappearance is a reliable indicator of malignant changes. Cartilage inside a fibrous dysplasia usually does not indicate malignant changes but only

Fig. 8.6 Different types and frequency of osteosarcomas in patients over age 65 (Istituto Ortopedico Rizzoli – Laboratory of Experimental Oncology – Section of Epidemiology – Bologna, Italy)
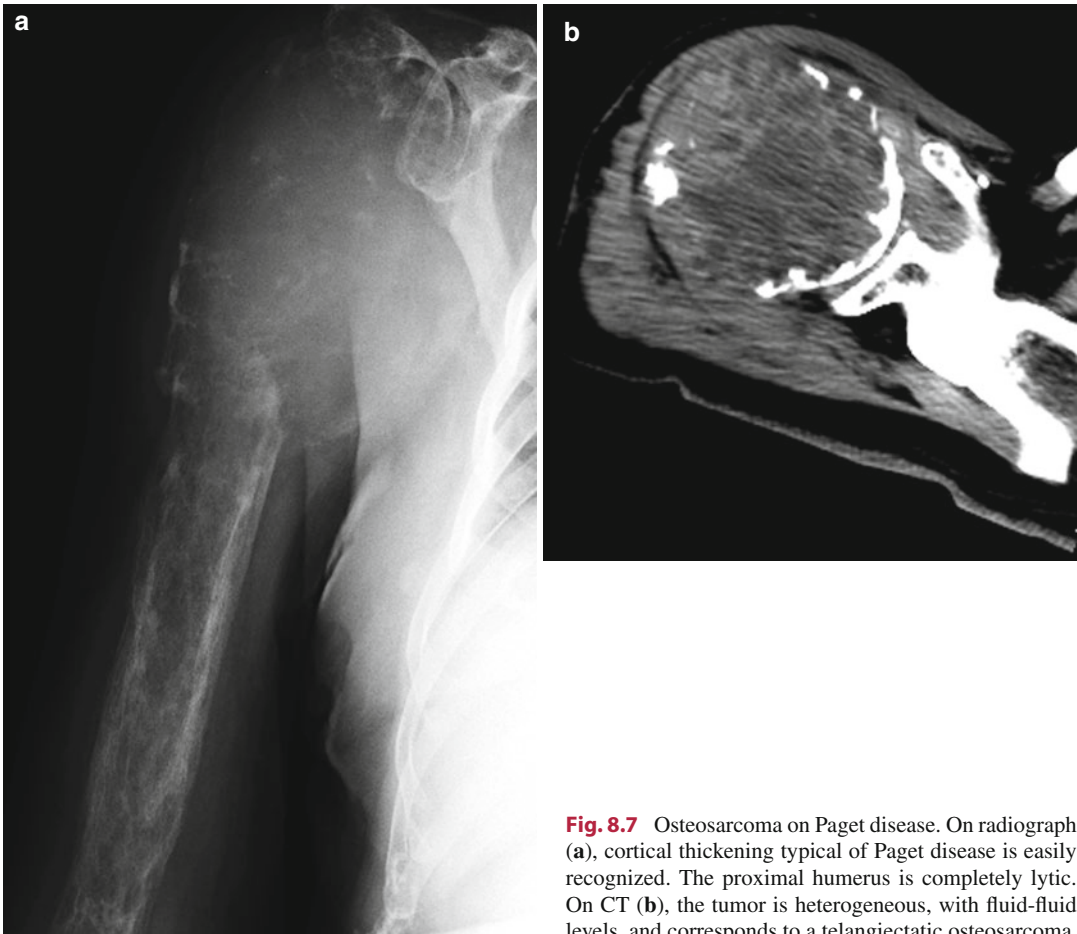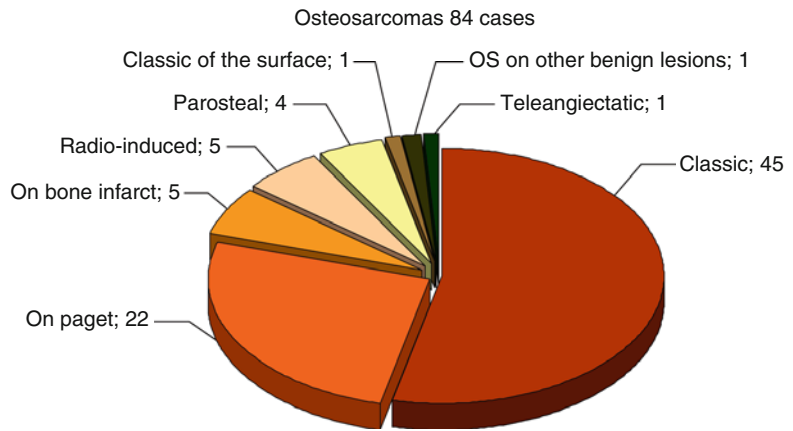

Osteosarcomas 84 cases

Classic of the surface; 1 — OS on other benign lesions; 1
Parosteal; 4 — Teleangiectatic; 1
Radio-induced; 5 — Classic; 45
On bone infarct; 5
On paget; 22

a

b

Fig. 8.7 Osteosarcoma on Paget disease. On radiograph (**a**), cortical thickening typical of Paget disease is easily recognized. The proximal humerus is completely lytic. On CT (**b**), the tumor is heterogeneous, with fluid-fluid levels, and corresponds to a telangiectatic osteosarcoma
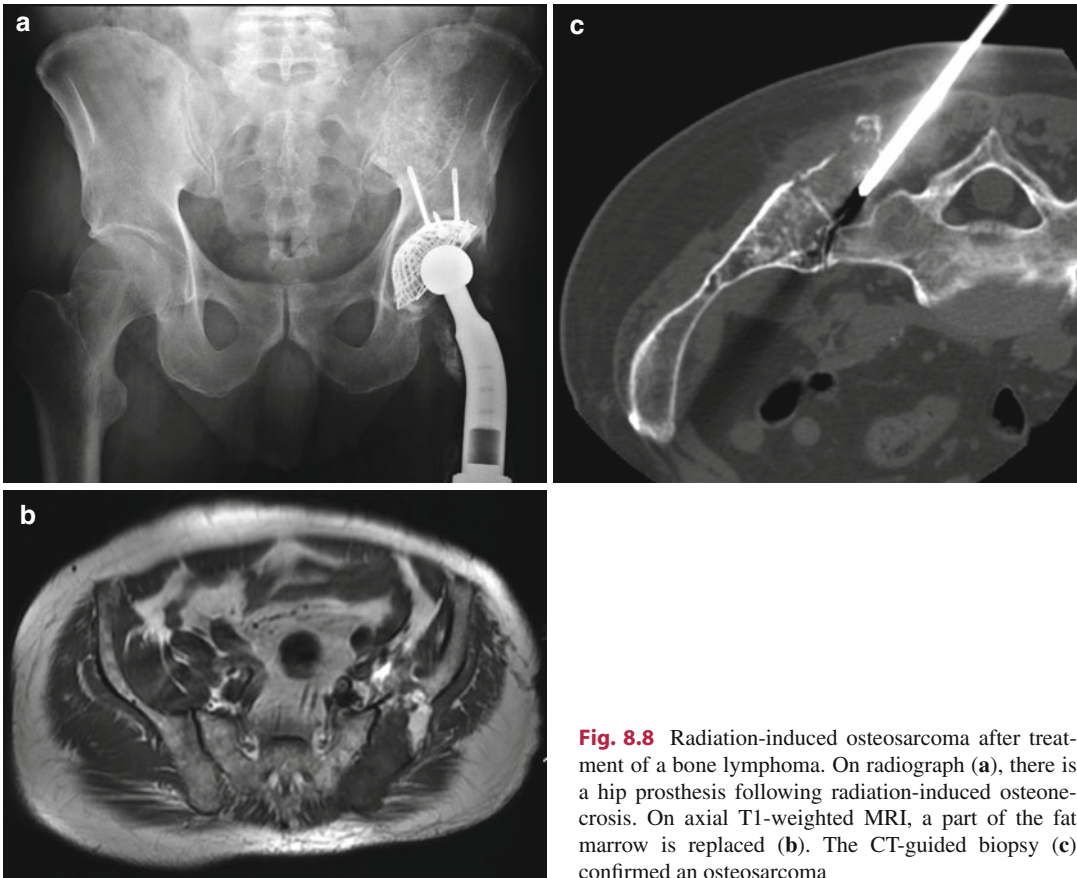
Fig. 8.8 Radiation-induced osteosarcoma after treatment of a bone lymphoma. On radiograph (**a**), there is a hip prosthesis following radiation-induced osteonecrosis. On axial T1-weighted MRI, a part of the fat marrow is replaced (**b**). The CT-guided biopsy (**c**) confirmed an osteosarcoma

a cartilaginous benign component inside the lesion.

- Fibrosarcoma is an aggressive, purely lytic, often metadiaphyseal tumor. It can also develop on an infarct.
- Chordoma involves the sacrum, clivus, and rarely mobile spine. Surgery is the only curative treatment. It is difficult in old patients. The lesion is lytic and often contains remaining pieces of bone. MR is the key examination for local staging, allowing à reliable prediction of the hazards and probable sequels (Fig. 8.9). Metastases are rare.
- Plasmocytoma is rare over 65 (Fig. 8.10). It is a purely lytic well-limited lesion, containing often thick trabeculae. Whole-body MR allows detection of minimal bone marrow lesions in

about half of the cases, allowing a general treatment. Myeloma (Fig. 8.11) has multiple, purely lytic, well-limited lesions. Evaluation of the tumor mass is still performed on radiographs, even if MR detects more lesions. Imaging helps follow the treatment and detect complications (Baur et al. 2002a; Lecouvet 2001).

8.2.4.2 Benign Tumors
They are incidental findings or are known for a long time. An asymptomatic chondroma is frequently discovered incidentally on MR performed for another reason in the knee or shoulder of a patient. A lesion centered in the medullary cavity without or with a limited cortical involvement and no soft tissue extension is very probably benign and does not require further examination.
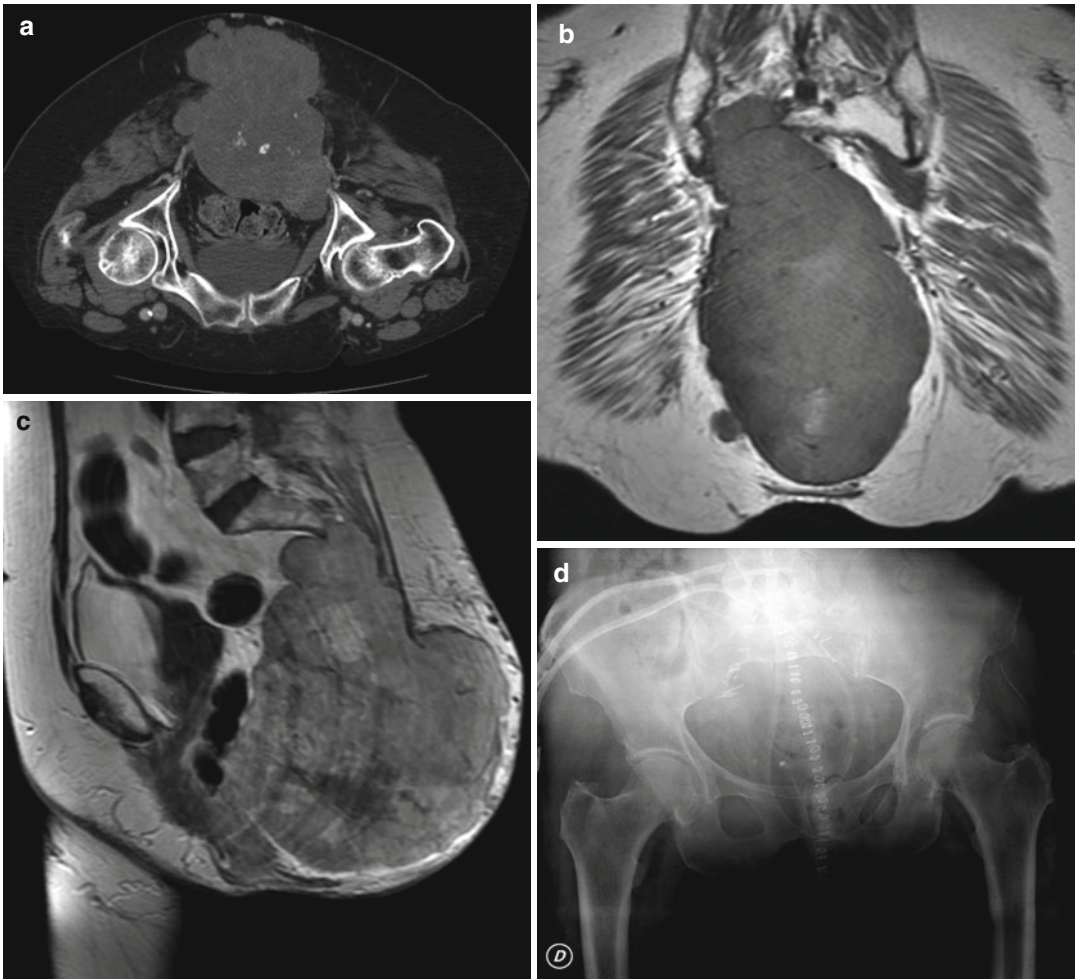
Fig. 8.9 Chordoma. On CT (**a**), the huge mass contains remaining pieces of bone. Coronal T1-weighted (**b**) and sagittal injected (**c**) images analyze the extension and allow a choice of level of resection. On the postoperative radiograph (**d**), S1 is preserved

Giant cell tumors can be found in the metaphyses of long bones and pelvis. They are purely lytic, well limited but without sclerosis. Denosumab may change their treatment. They may rarely develop in Paget disease.

8.3 Metastases

8.3.1 Introduction

They are by far the most frequent bone tumors in old patients. Imaging should be used for routine screening in tumors with a high incidence of bone metastases such as breast and prostate cancer, if and only if there are practical consequences (Boccardo et al. 1995; Rosselli Del Turco et al. 1994). It is used in symptomatic patients presenting with pain or neurological deficit, and it is mandatory before aggressive surgery (pneumonectomy, prostatectomy, cystectomy, amputation, etc.), when their discovery may change the surgical approach. For these purposes, imaging includes radiographs, radionuclide scintigraphy, CT, MRI, and PET.

Most bone metastases are asymptomatic. Over 90 % occur within the red marrow (Silverberg and Lubera 1987; Abrams et al.
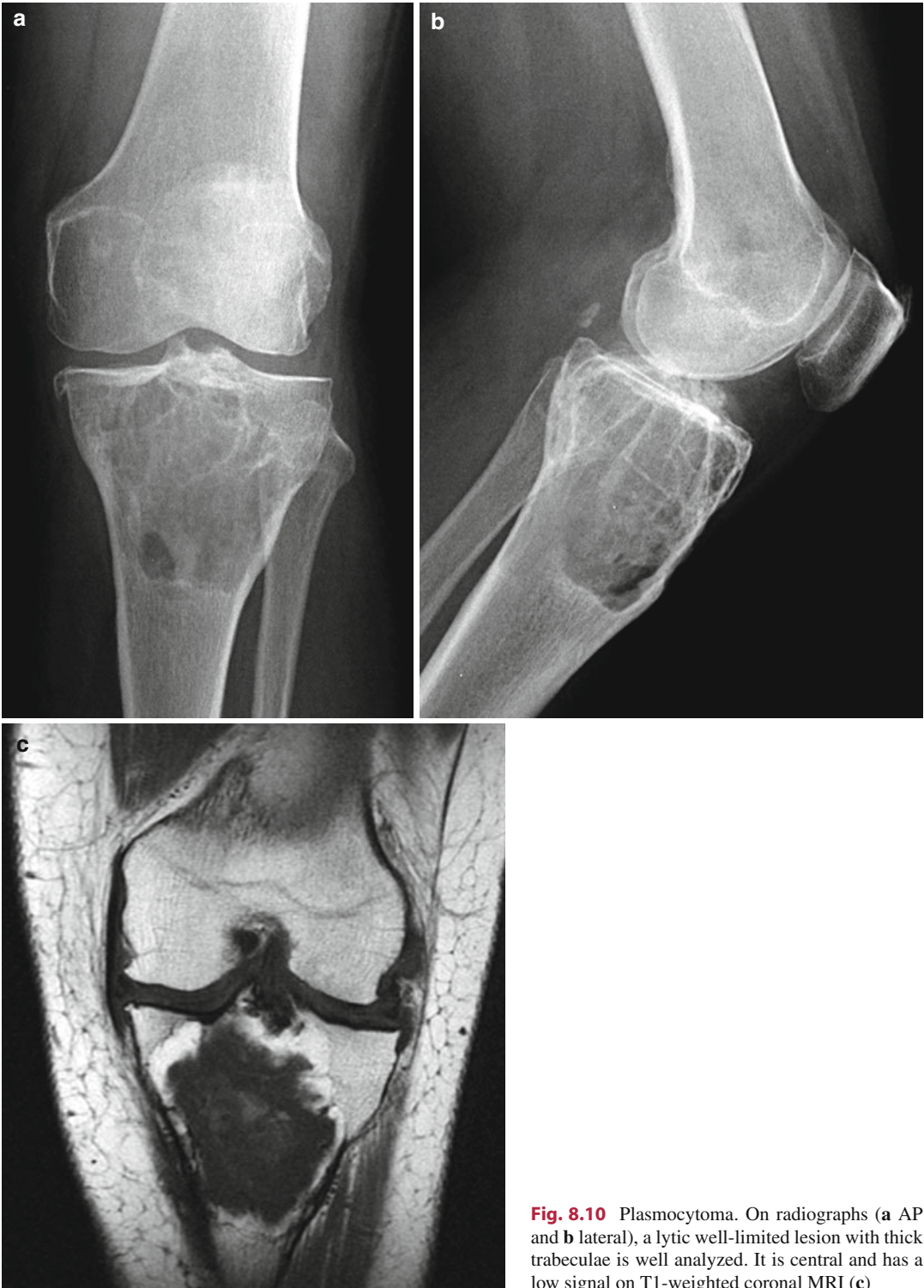
Fig. 8.10 Plasmocytoma. On radiographs (**a** AP and **b** lateral), a lytic well-limited lesion with thick trabeculae is well analyzed. It is central and has a low signal on T1-weighted coronal MRI (**c**)

Fig. 8.11 Myeloma. Sagittal T1-weighted images (**a**), showing minimal femoral and tibial lesions, considered as traumatic. Three months later, fracture and lytic tibial and femoral lesions, on radiograph (**b**), sagittal T1 (**c**), and T2-weighted (**d**) images

1950; Krishnamurthy 1977). That explains why systematic detection looks mainly at the spine, pelvis, and proximal long bones. Approximately 10 % of metastases are solitary, which may rarely have practical treatment consequences: an isolated bone metastasis can be cured in 40 % of kidney cancers, but not in a breast cancer. Extraskeletal spread into the soft tissues is rare (Wyche and De Santos 1978). Special imaging features can guide the search of a primary

unknown cancer: distal metastases (Fragiadakis and Panayotopoulous 1972) and cortical bone metastases most frequently occur in lung cancer (Deutsch and Resnick 1980), metastases expanding the bone in kidney and thyroid cancer. Metastatic cancer to the skeletal bone occurs in 30–70 % of all cancer patients (Bloem et al. 1988; Bohndorf et al. 1986) Breast and prostate cancers are the most common causes of bone metastases. Overall breast cancer is responsible for approximately 70 % of all bone metastases in women and prostate cancer represents the primary cause in 60 % of bone metastases in men (Schima et al. 1994).

8.3.2 Imaging Techniques

Radiographs are mainly used to study a painful lesion, especially a fracture, as they are poorly sensitive but rather specific.

8.3.2.1 Radionuclide Scintigraphy
Bone may be imaged using Tc-99m diphosphonate scanning, which images the whole body. It detects metastatic lesions before they are visible on plain radiographs: good sensitivity but low specificity (Fig. 8.12). It is less efficient in purely lytic lesions. Radionuclide bone scans are relatively insensitive for evaluating treatment response. However, in 10–15 % of patients, a "flare phenomenon" is seen, with increased bony uptake due to stimulation of osteoblastic activity in response to treatment (Fragiadakis and Panayotopoulous 1972; Kattapuram et al. 1990).

8.3.2.2 Computed Tomography
CT provides guidance for percutaneous bone biopsy and imaging-guided treatment (Fig. 8.13). Lesions are often detected on a CT performed for a global evaluation of a cancer, but MR sensitivity for bone is by far superior (Fig. 8.14). CT is used when MR is contraindicated.

8.3.2.3 Magnetic Resonance Imaging
MRI has excellent spatial and contrast resolution, multiplanar imaging capability, and the unique ability to separate hemopoietic (red) marrow from non-hemopoietic (yellow) marrow. It also provides the opportunity to survey large volumes of bone marrow at a single examination. It is highly sensitive for the detection of bone marrow metastases, demonstrating lesions even when normal radiographs and negative radionuclide bone scans fail to do so (Traill et al. 1999; Kattapuram et al. 1990; Algra et al. 1991). It is still more efficient in old patients, because of the high contrast between fat marrow and metastases. Not uncommonly, MRI demonstrates incidental bone marrow metastases in patients undergoing MRI for primary tumor staging. The opportunity to study the whole skeleton on a single MR examination in a reasonable time (around 20 min) makes MR even more

Fig. 8.12 Metastases of prostate cancer. On sagittal CT (**a**), multiple lytic metastases with vertebral collapses are seen. Bone scintigraphy (**b**) gives a global view of the lesions

Fig. 8.12 (continued)
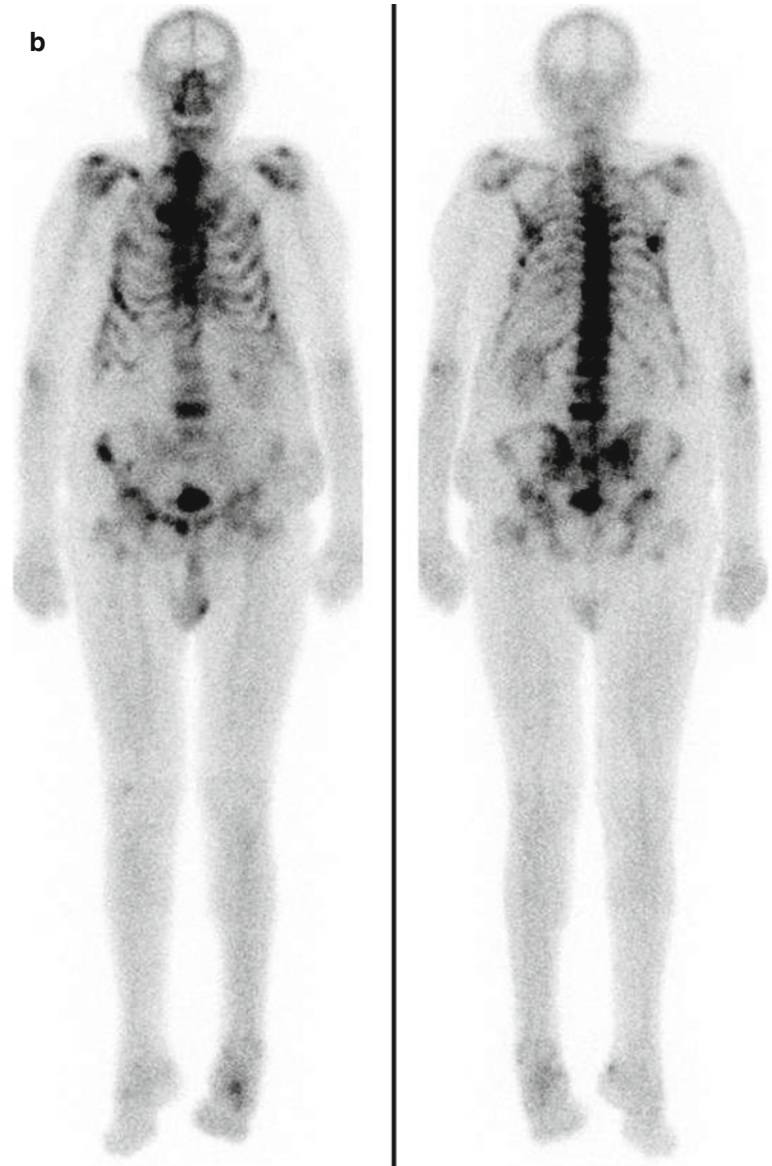
efficient (Eustace et al. 1997; Lauenstein et al. 2002). The appearance of the bone marrow on MRI depends on a number of factors including mineral, fat, and water composition.

MR Sequences

Fat and water distribution in bone marrow (normal marrow always containing fat and water and metastases water only), indirect visualization of normal bone trabeculae on gradient-echo images, indirect evaluation of bone edema and cell density on diffusion, and the study of vascularization can be ingeniously combined to enable good detection and characterization of lesions (Vanel et al. 1998).

Fat and Water

Normal marrow contains both fat and water (yellow marrow 80 % fat, but also 15 % water). In infiltrative disorders, fat disappears. Sequences
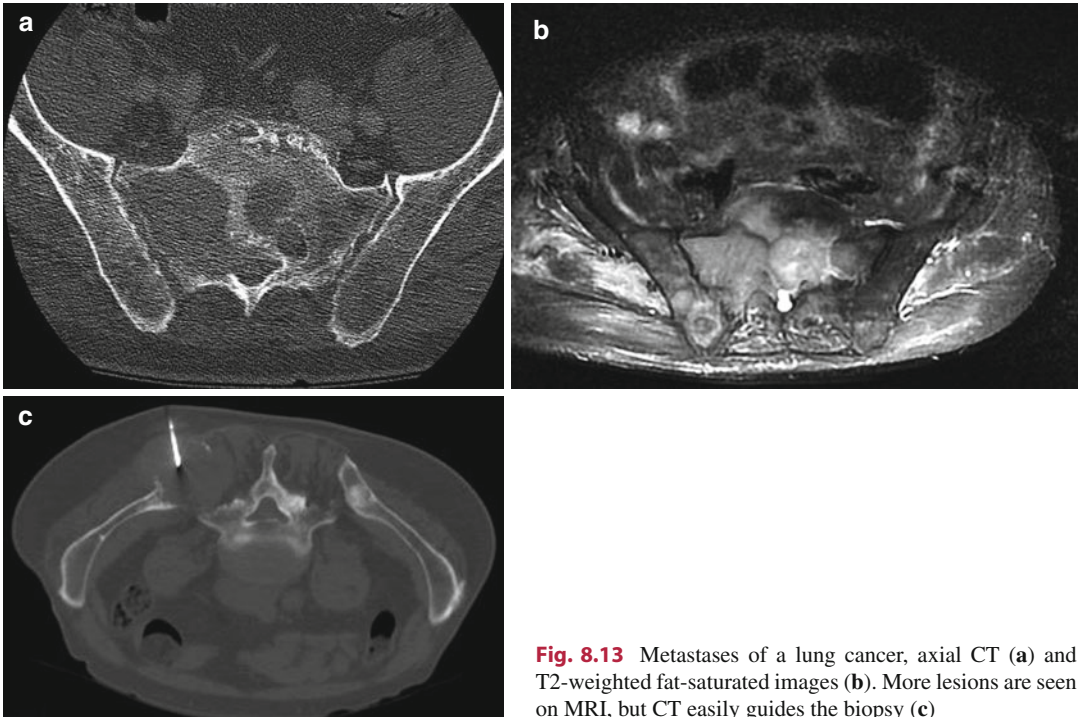
Fig. 8.13 Metastases of a lung cancer, axial CT (**a**) and T2-weighted fat-saturated images (**b**). More lesions are seen on MRI, but CT easily guides the biopsy (**c**)

displaying differences between fat and water signal are thus useful.

T1-Weighted Spin-Echo Sequences

Fat has a higher signal than water and the highest signal. Thus, fatty marrow containing 80 % fat exhibits a high signal intensity and any focal lesion showing a lower signal intensity is easy to detect. This is why this sequence is very useful and usually the first used (Fig. 8.14).

Chemical Shift Imaging

The difference in resonance frequency between water and fat protons can be used. It has no consequence on the contrast with conventional spin-echo sequences as the 180° pulse cancels the difference. By shifting the readout window, it is possible to obtain images in which contrast is related to the difference between the quantities of water and fat protons (opposed-phase images).

In gradient-echo sequences, the same phenomenon occurs, depending only on the echo time. If fat and water protons are in phase, their signals are added; if they are in opposed phase, they are subtracted. If a lesion replaces normal marrow, fat can be obliterated, and no subtraction will occur. The difference between the signal produced by normal marrow, which always contains water and fat, will be emphasized on opposed-phase sequences.

Fat Suppression Techniques

A 180° inversion pulse is used initially for STIR (short tau inversion recovery) sequences. The inversion time is chosen to cancel the signal of fat. This sequence can be obtained on any MR unit, but it cancels every signal identical to fat, for example, blood in hematoma or contrast-enhanced tissue. The difference between fat and water proton frequency is also used for fat presaturation. A saturation pulse with a narrow band at the exact fat frequency is used before the usual pulse. A very homogeneous magnetic field is required; therefore, this sequence is more specific, but not effective on every unit.
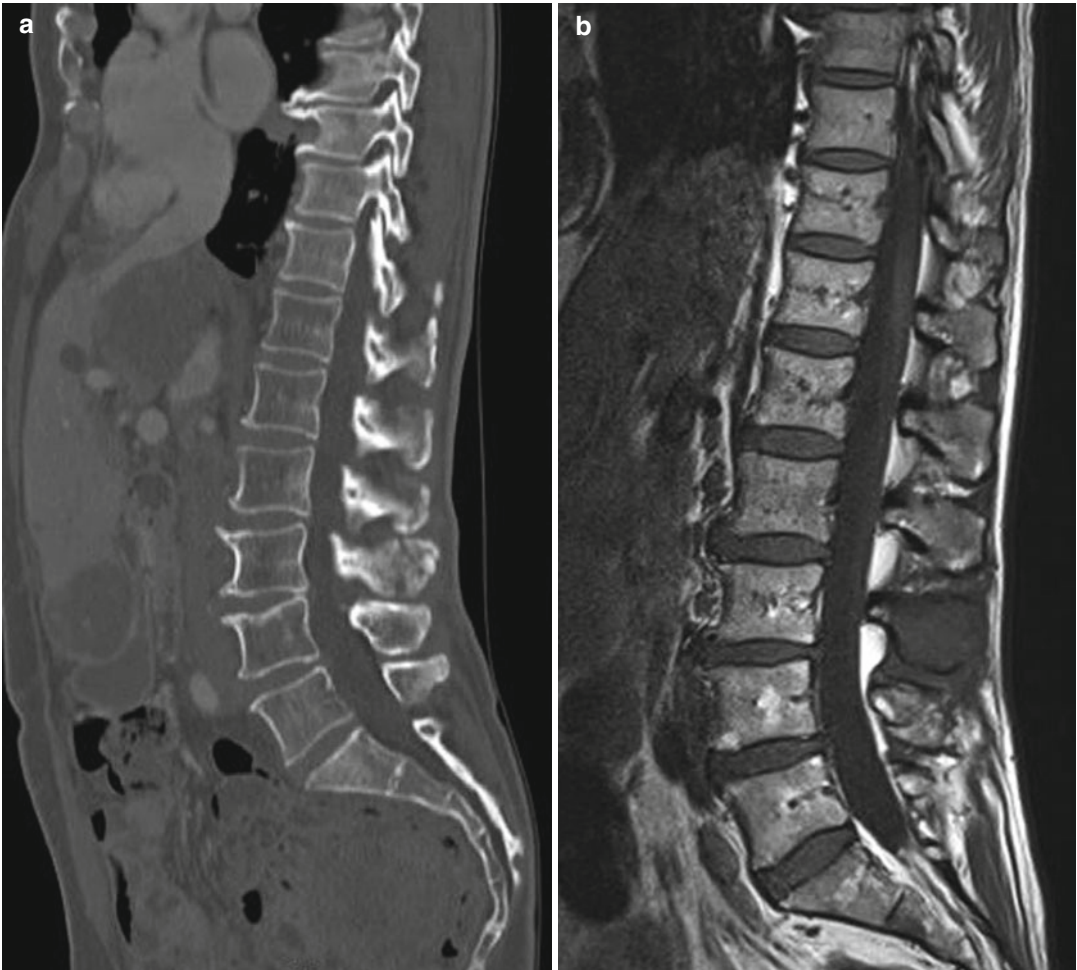
Fig. 8.14 Metastases of a colon cancer, sagittal CT (**a**) and T1-weighted MRI (**b**). The lesion of the spinous process of L3 is much easier to detect on MRI

Bone Trabeculae

Because of the lack of mobile protons, trabecular bone yields no detectable signal but creates magnetic field heterogeneities. These have minimal impact on spin-echo sequences, as their effect is cancelled by the 180° pulse, but there may be a visible effect on gradient-echo sequences as field heterogeneity is not cancelled. If the echo delay time is long enough, the signal can be decreased considerably because of the presence of normal trabeculae. This is particularly visible in the vertebrae, pelvic bones, and the proximal ends of the long tubular bones. If bone trabeculae have been destroyed, the signal will be higher than in the preserved parts of the bone. Thus, this provides an indirect technique for the diagnosis of trabecular lysis.

Diffusion

Diffusion imaging is difficult to apply on the spine because the signal is weak. When multiple cellular walls prevent diffusion (e.g., when tumor cells are tightly packed), the signal is higher than in areas of edema or necrosis, where diffusion readily occurs (Baur et al. 1998, 2002b).

Contrast Medium

After injection of gadolinium chelates, changes in the signal of normal marrow are not visible

Fig. 8.15 Metastases of a melanoma, with a compression; sagittal T2-weighted images of the lumbar (**a**) and thoracic (**b**) spine. Multiple compression levels are well seen: L3, T12 but also a higher thoracic lesion. The surgeon must know all lesions before making any therapeutic choice

on T1-weighted images and measurements display either no increase or only a limited increase. Various pathologies, in contrast, usually exhibit a strong signal increase. The absence of uptake practically rules out involvement of the bone marrow. Uptake is usually evaluated on T1-weighted sequences with fat presaturation.

Metastatic lesions are typically focal with low signal on T1-weighted images and higher signal intensity (greater than marrow fat) on T2-weighted sequences. On fast spin-echo T2-weighted fat-saturated sequences, lesions are often of very high signal, particularly lytic metastases. Sclerotic lesions are of low signal intensity on T1- and T2-weighted images, typically seen in metastases from prostate and breast cancer. A third pattern is a diffuse inhomogeneous low signal involving the whole bone. Rarely, a diffuse homogeneous low signal is seen on T1-weighted images and homogeneous increased signal is seen on T2-weighted images.

Metastases enhance following injection of intravenous contrast material.

When a potentially operable vertebral compression is discovered on an MR examination, the whole spine must be studied to rule out another level of compression, which could change patient management (Fig. 8.15).

If no abnormality is detected on an MRI performed for a suspected cord compression, contrast medium must be used to detect leptomeningeal metastases.

Evaluation of Vertebral

Osteoporotic vertebral collapses are frequent in old patients, and differentiating metastatic collapses may be very useful (Laredo et al. 1995).

Imaging features suggestive of malignant vertebral collapse are involvement of the posterior vertebral body and posterior elements, associated soft tissue mass, diffuse involvement of the whole vertebra, and contrast enhancement of the abnormal area and multiple lesions.

Direct signs bring a higher specificity in the analysis of vertebral collapse. They use

diffusion and gradient-echo techniques. On diffusion-weighted sequences, protons diffuse in the free water of osteoporotic vertebral collapse, and thus, the signal intensity is reduced. Conversely, diffusion is limited by the walls of the tumor cells in metastatic vertebral collapse, and thus, a higher signal intensity is maintained.

On in-phase gradient-echo images, the lack of trabeculae in metastatic collapse allows a higher

Fig. 8.16 Metastases of a breast cancer. On radiograph (**a**), multiple scler otic metastases are easily detected. On sagittal T1-weighted images, without (**b**) and with (**c**) contrast medium injection, massive involvement of the marrow is visible. On PET-CT (**d**), involvement of the whole spine as well as ribs and pelvis is detected
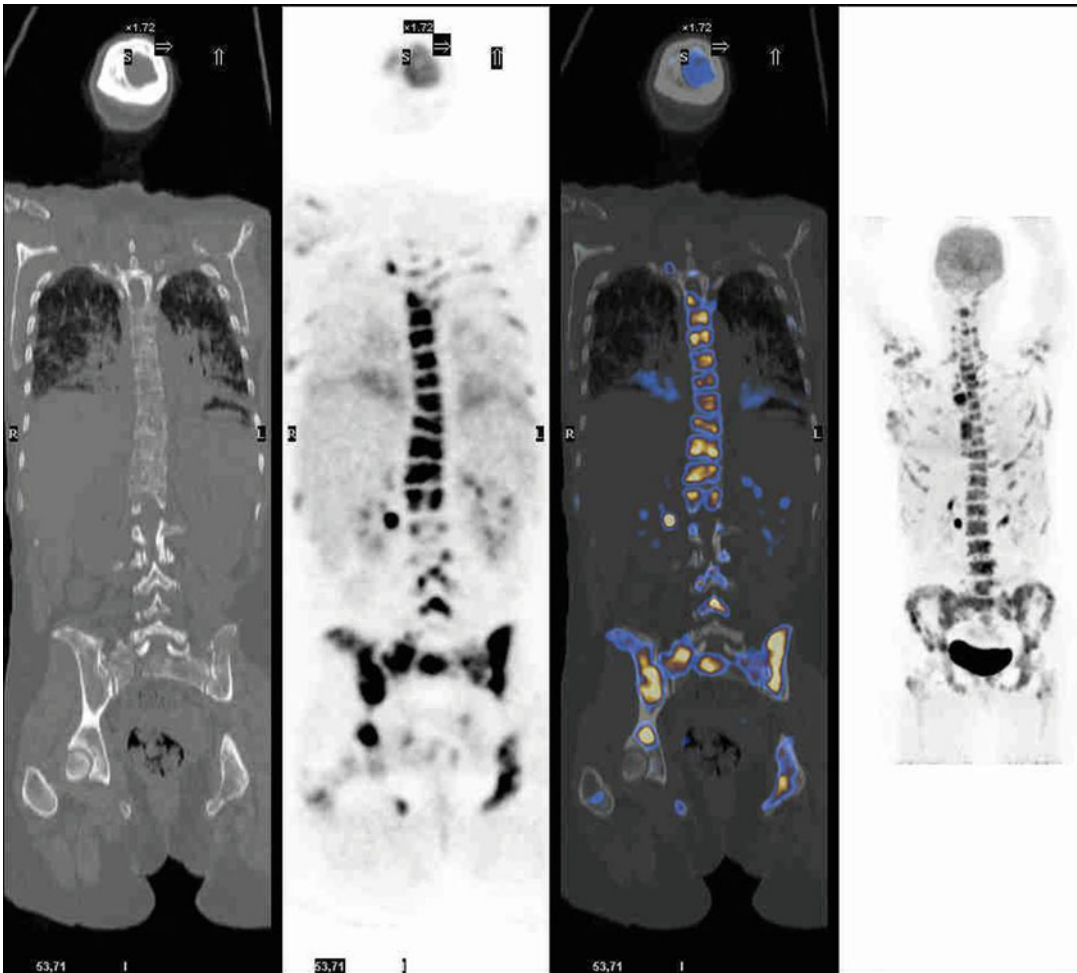
Fig. 8.16 (continued)

signal, whereas the preserved trabeculae in osteoporotic collapse make the signal low.

Monitoring Tumor Response to Treatment

Tumors in bone marrow respond to treatment with a reduction in size and a change in signal intensity. Changes in lesion size are best demonstrated on T1-weighted images, but signal intensity changes are often better appreciated on T2-weighted or STIR images. When treatment is effective, a fatty halo may appear, marking a decrease in tumor size. When, after radiation therapy, the marrow becomes completely fatty, there are no lesions left. Most often, after radiation or chemotherapy, lesions are still visible. Differentiation between fibrosis and viable tumor is not possible, and MRI is not recommended to evaluate treatment effectiveness.

After spine surgery, a medial sagittal MRI can be obtained, if surgical fixation is lateral (transpedicular) and titanium is used.

8.3.2.4 PET with Fluorodeoxyglucose (^{18}FDG-PET)

^{18}FDG-PET produces metabolic images, most often linked to glucose taken up by the tissues, and although a promising technique, it is still under investigation for bone metastases (Fig. 8.16). Sclerotic metastases are poorly detected on PET alone, but the CT part of the examination renders their diagnosis possible.

> **Conclusion**
>
> In old patients, metastases are by far the most frequent bone tumors. They must be detected when such knowledge will change the treatment. Bone scintigraphy allows a simple global evaluation, MRI is more sensitive, and CT helps guide interventional radiology.
>
> In primary tumors, diagnosis depends first on radiographs; CT is used in flat and short bones, and MRI gives the best local staging, allowing planning for curative surgery.

References

Abrams HL, Spiro R, Goldstein N (1950) Metastases in carcinoma. Analysis of 1000 autopsied cases. Cancer 2:74–85

Aisen AM, Martel W, Braunstein EM, McMilin KI, Philips WA, Kling TF (1986) MRI and CT evaluation of primary bone and soft tissue tumors. AJR Am J Roentgenol 146:749–756

Algra PR, Bloem JL, Tissing H et al (1991) Detection of vertebral metastases: comparison between MR imaging and bone scintigraphy. Radiographics 11:219–232

Baur A, Stabler A, Bruning R et al (1998) Diffusion-weighted MR imaging of bone marrow: differentiation of benign versus pathologic compression fractures. Radiology 207:349–356

Baur A, Stäbler A, Nagel D, Lamerz R, Bartl R, Hiller E, Wendtner C, Bachner F, Reiser M (2002a) Magnetic resonance imaging as a supplement for the clinical staging system of Durie and Salmon? Cancer 95(6):1334–1345

Baur A, Dietrich O, Reiser M (2002b) Diffusion-weighted imaging of the spinal column. Neuroimaging Clin N Am 12(1):147–160

Bloem JL, Taminiau AHM, Eulderink F, Hermans J, Pauwels EKJ (1988) Radiologic staging of primary bone sarcoma. MRI, scintigraphy, angiography and CT correlated with pathologic examination. Radiology 169:805–810

Boccardo F, Bruzzi P, Cionini L et al (1995) Appropriateness of the use of clinical and radiologic examinations and laboratory tests in the follow-up of surgically-treated breast cancer patients. Results of the Working Group on the Clinical Aspects of Follow-up. Ann Oncol 6(Suppl 2):57–59

Bohndorf K, Reiser M, Lochner B, Feaux de Lacroux W, Steinbrich W (1986) Magnetic resonance imaging of primary tumors and tumor like lesions of bone. Skeletal Radiol 15:511–517

Brown KT, Kattapuram SSV, Rosentahl DI (1986) Computed tomography analysis of bone tumors: patterns of cortical destruction and soft tissue extension. Skeletal Radiol 15:448–451

De Baere T, Vanel D, Shapeero LG, Charpentier A, Terrier P, Di Paola M (1992) Osteosarcoma after chemotherapy: evaluation with contrast material-enhanced subtraction MR imaging. Radiology 185:587–592

Deutsch A, Resnick D (1980) Eccentric cortical metastases to the skeleton from bronchogenic carcinoma. Radiology 137:49–52

Eustace S, Tello R, DeCarvalho V et al (1997) A comparison of whole-body turbo STIR MR imaging and planar 99mTc-methylene diphosphonate scintigraphy in the examination of patients with suspected skeletal metastases. Am J Roentgenol 169:1655–1661

Fragiadakis EG, Panayotopoulous G (1972) Metastatic carcinoma of the hand. Hand 4:268

Geirnaerdt MJ, Hogendoorn PC, Bloem JL, Taminiau AH, van der Woude HJ (2000) Cartilaginous tumors: fast contrast-enhanced MR imaging. Radiology 214(2):539–546

Glass RB, Poznanski AK, Fisher MR, Shkolnik A, Dias L (1986) MR imaging of osteoid osteoma. J Comput Assist Tomogr 10:1065–1067

Kattapuram SV, Khurana JS, Scott JA et al (1990) Negative scintigraphy with positive magnetic resonance imaging in bone metastases. Skeletal Radiol 19:113–116

Kenney PJ, Gilula LA, Murphy WA (1981) The use of CT to distinguish osteochondroma and chondrosarcoma. Radiology 138:129–137

Krishnamurthy GT, Tubis M, Hiss J et al (1977) Distribution pattern of metastatic bone disease. A need for total body skeletal image. JAMA 237:2504–2506

Laredo JD, Lakhdari K, Bellaiche L et al (1995) Acute vertebral collapse: CT findings in benign and malignant non-traumatic cases. Radiology 194:41–48

Lauenstein TC, Freudenberg LS, Goehde SC et al (2002) Whole-body MRI using a rolling table platform for the detection of bone metastases. Eur Radiol 12:2091–2099

Lecouvet FE, Vande Berg BC, Malghem J, Maldague BE (2001) Magnetic resonance and computed tomography imaging in multiple myeloma. Semin Musculoskelet Radiol 5(1):43–55, Review

Lodwick GS, Wilson AJ, Farrel C, Virtama P, Smeltzer FM, Ditrich F (1980) Estimating rate of growth in bone lesions: observer performance and error. Radiology 134:585–590

Madewell JE, Ragsdale BD, Sweet DE (1981) Radiology and pathology analysis of solitary bone lesions. Radiol Clin North Am 19:715–748

Murphey MD, Flemming DJ, Boyea SR, Bojescul JA, Sweet DE, Temple HT (1998) Enchondroma versus chondrosarcoma in the appendicular skeleton: differentiating features. Radiographics 18(5):1213–1237; quiz 1244–1245

Picci P, Vanel D, Briccoli A, Talle K, Haakenaasen U, Malaguti C, Monti C, Ferrari C, Bacci G, Saeter G, Alvegard TA (2001) Computed tomography of pulmonary metastases from osteosarcoma: the less poor technique. A study of 51 patients with histological correlation. Ann Oncol 12(11):1601–1604

Regent D, Tamisier JN, Fery A, Bernard C, Delagoutte JP, Pourel JP, Gaucher A (1986) Intérêt du traitement de l'information dans l'exploration scanographique des lésions focales bénignes de l'os. Rev Rhum Mal Osteoartic 53:77–82

Rosselli Del Turco M, Palli D, Cariddi A, Ciatto S, Pacini P, Distante V (1994) Intensive diagnostic follow-up after treatment of primary breast cancer. A randomized trial National Research Council Project on Breast Cancer follow-up. JAMA 271:1593–1597

Schima W, Amann G, Stiglbauer R et al (1994) Preoperative staging of osteosarcoma: efficacy of MR imaging in detecting joint involvement. AJR Am J Roentgenol 163:1171–1175

Shaylor PJ, Peake D, Grimer RJ, Carter SR, Tillman RM, Spooner D (1999) Paget's osteosarcoma – no cure in sight. Sarcoma 3(3–4):191–192

Silverberg E, Lubera J (1987) Cancer statistics, 1987. CA Cancer J Clin 37:2–19

Staals EL, Bacchini P, Bertoni F (2006) Dedifferentiated central chondrosarcoma. Cancer 106(12):2682–2691

Staals EL, Bacchini P, Mercuri M, Bertoni F (2007) Dedifferentiated chondrosarcomas arising in preexisting osteochondromas. J Bone Joint Surg Am 89(5): 987–993

Traill ZC, Talbot D, Golding S et al (1999) Magnetic resonance imaging versus radionuclide scintigraphy in screening for bone metastases. Clin Radiol 54:448–451

van der Woude HJ, Bloem JL, Holscher HC, Nooy MA, Taminiau AH, Hermans J, Falke TH, Hogendoorn PC (1994) Monitoring the effect of chemotherapy in Ewing's sarcoma of bone with MR imaging. Skeletal Radiol 23(7):493–500

Vanel D, Henri-Amar M, Lumbroso J, Lemalet E, Couanet D, Piekarski JD, Masselot J, Boddaert A, Kalifa C, Le Chevalier T, Lemoine G (1984) Pulmonary evaluation of patients with osteosarcoma: roles of standard radiography, tomography, CT, scintigraphy and tomoscintigraphy. AJR Am J Roentgenol 143:519–523

Vanel D, Bittoun J, Tardivon A (1998) MRI of bone metastases. Eur Radiol 8:1345–1351

Vanel D, Kreshak J, Larousserie F, Alberghini M, Mirra J, De Paolis M, Picci P (2012) Enchondroma vs. chondrosarcoma: a simple, easy-to-use, new magnetic resonance sign. Eur J Radiol [Epub ahead of print]

Verstraete KL, De Deene Y, Roels H et al (1994) Benign and malignant musculoskeletal lesions: dynamic contrast-enhanced MR imaging parametric "first-pass" images depict tissue vascularization and perfusion. Radiology 192:835–843

Wyche LD, De Santos LA (1978) Spiculated periosteal reaction in metastatic disease resembling osteosarcoma. Orthopedics 1:215